dr Ireneusz Grulkowski
Instytut Fizyki
Uniwersytet Mikołaja Kopernika w Toruniu
ul. Grudziądzka 5
87-100 Toruń

Załącznik nr 3 do wniosku o przeprowadzenie postepowania habilitacyjnego

Autoreferat (w języku angielskim)

Scientific curriculum vitae and presentation of scientific achievements (in English)

I. Name and surname:

Ireneusz Paweł Grulkowski

II. Scientific degrees:

2007 **Ph.D. in Physics** (degree with honourable mention – summa cum laude); Faculty of Mathematics, Physics and Computer Science; University of Gdańsk; Gdańsk, supervisor: Prof. Piotr Kwiek
Title of thesis: *Light diffraction by cylindrical ultrasonic waves*.

2005 **M. Sc. in Biotechnology**; Intercollegiate Faculty of Biotechnology of University of Gdańsk and Medical University of Gdańsk; Gdańsk, supervisor: Dr. Agnieszka Kowalska
Title of thesis: *Formation of protoporphyrin IX in HeLa cells incubated with 5-aminolevulinic acid and its esters*.

2003 **M. Sc. in Biomedical Physics**; Faculty of Mathematics, Physics and Computer Science; University of Gdańsk; Gdańsk, supervisor: Prof. Piotr Kwiek
Title of thesis: *Acousto-optic lens as a scanner in optical coherence tomography (OCT)*.

III. Academic positions:

2008- Institute of Physics; Nicolaus Copernicus University in Toruń (Assistant Professor)

2010-2012 Research Laboratory of Electronics; Massachusetts Institute of Technology (Visiting Scientist)

2008-2010 Institute of Experimental Physics; University of Gdańsk (Assistant Professor)

IV. Summary of scientific record (publications and presentations):

Scientific record	Before PhD completion	After PhD completion	Total
Publications, including:	**13**	**47**	**60**
- Chapters in books	0	4	4
- Articles in peer-reviewed journals in Journal Citation Reports (with Impact Factor)	5	26	31
- Articles in peer-reviewed journals not listed in Journal Citation Reports (w/o Impact Factor)	2	1	3
- Conference proceedings (not peer-reviewed)	6	16	22
Presentations, including:	**9**	**79**	**88**
- Invited lectures at conferences	2	6	8
- Regular oral presentations at conferences	7	45	52
- Regular poster presentations at conferences	0	23	23
- Invited presentations in other research centers	0	5	5

V. Indication of scientific achievement following article 16 par. 2 of act from 14 March 2003 on scientific degrees and scientific title and on degrees and title in arts (Journal of Laws no. 65, pos. 595 with changes.):

(a) Title of the scientific achievement:

I do indicate that the scientific achievement following art. 16 par. 2 of the Act on Scientific Degrees and Titles from March 14th, 2003, consists of a series of publications focused on subject of quantitative eye imaging and extraction of parameters of optical elements based optical coherence tomography (OCT) data. The achievement has been entitled as:

Infrared interferometric imaging– comprehensive biometry of the eye and microprofilometry

(b) List of papers presenting the scientific achievement:

The scientific achievement has been demonstrated in the publications, the list of which is given below (numeration as in Annex 4; personal contribution described in Annex 4):

[I.B.1] I. Grulkowski, M. Góra, M. Szkulmowski, D. Szlag, S. Marcos, A. Kowalczyk, M. Wojtkowski, Comprehensive anterior segment imaging using Spectral OCT system with high-speed CMOS camera, *Opt. Express* **17** (2009), 4842-4858.

IF: 3.278, times cited: 99, estimated contribution: 50%.

[I.B.2] I. Grulkowski, I. Gorczyńska, M. Szkulmowski, D. Szlag, A. Szkulmowska, R. A. Leitgeb, A. Kowalczyk, M. Wojtkowski, Scanning protocols dedicated to smart velocity ranging in Spectral OCT, *Opt. Express* **17** (2009), 23736-23754.

IF: 3.278, times cited: 64, estimated contribution: 50%.

[I.B.3] I. Grulkowski, J. J. Liu, B. Potsaid, V. Jayaraman, Ch. D. Lu, J. Jiang, A. E. Cable, J. S. Duker, J. G. Fujimoto, Retinal, anterior segment and full eye imaging using ultrahigh speed swept source OCT with vertical-cavity surface emitting lasers, *Biomed. Opt. Express* **3** (2012), 2733-2751.

IF: 3.176, times cited: 98, estimated contribution: 40%.

[I.B.4] I. Grulkowski, J. J. Liu, J. Y. Zhang, B. Potsaid, V. Jayaraman, A. E. Cable, J. S. Duker, J. G. Fujimoto, Reproducibility and repeatability of novel optical ocular biometry using long-range swept source OCT imaging with VCSEL technology, *Ophthalmology* **120** (2013), 2184-2190.

IF: 6.17, times cited: 11, estimated contribution: 50%.

[I.B.5] I. Grulkowski, J. J. Liu, B. Potsaid, V. Jayaraman, J. Jiang, A. E. Cable, J. G. Fujimoto, High precision, high accuracy ultralong range swept source OCT using VCSEL light source, *Opt. Lett.* **38** (2013), 673-675.

IF: 3.179, times cited: 42, estimated contribution: 40%.

[I.B.6] K. Karnowski, I. Grulkowski, N. Mohan, I. Cox, M. Wojtkowski, Quantitative optical inspection of contact lenses immersed in wet cell using swept source OCT, *Opt. Lett.* **39** (2014), 4727-4730.

IF: 3.292, times cited: 3, estimated contribution: 30%.

(c) Description of scientific aims, achieved results and possible applications:

Infrared interferometric imaging– comprehensive biometry of the eye and microprofilometry

V.1. Introduction and motivation

Infrared interferometric techniques have been widely used in many branches of science and technology. Firstly, Fourier transform infrared spectroscopy (FTIR) is nowadays a common spectroscopic method for chemical analysis [1]. Moreover, with an array of telescopes operating effectively as an interferometer at near infrared radiation, it is possible to perform astronomical observations with higher resolution [2]. In addition to that, many near-infrared remote sensing technologies are based on interferometry [3]. Biomedical imaging using low-coherence interferometry in the near infrared wavelength region is currently rapidly developing field offering unprecedented insight into structure and functions of biological objects.

The human eye is a complex and dynamic optical structure enabling visual perception, i.e. conversion of light into electrical signals that are later processed by the brain. Anatomically, the front of the eye constitutes its anterior segment and includes the elements spanning from the cornea to the posterior surface of the crystalline lens. Therefore, from the physical (optical) point of view, the anterior segment of the eye is composed of the optical elements of different refractive properties, thus forming a compound optical system.

Inspection of anterior segment structures is an integral part of ophthalmic examination. In particular, imaging of the anterior segment of the eye is a common clinical procedure in the diagnosis and surgical management of ocular disorders such as glaucoma and cataract. It also aims at evaluation of clinically relevant features of the anterior segment of the eye in a variety of eye conditions. Moreover, visualization and quantitative description of the anterior segment of the eye reveals refractive status of the eye, thus playing an important role in efficient vision correction (e.g. lens fitting) or refractive surgery.

In clinical practice, imaging of the anterior segment has been traditionally carried out with slit lamp biomicroscopy. However, anterior segment imaging is currently a rapidly advancing field of ophthalmology and provides tools that supplement well-established modalities. Those modern techniques include ultrasound biomicroscopy, confocal microscopy, Scheimpflug imaging, corneal topography etc. Apart from instrumentation development, a tremendous effort has been made to implement image analysis techniques which allow obtaining quantitative information on the state of the cornea, anterior chamber, corneo-scleral angle and the crystalline lens. Consequently, application of new technologies for *in vivo* imaging significantly improves clinical procedures in ophthalmology [II.D.1].

One of the main breakthrough developments in eye diagnostics was the introduction of optical coherence tomography (OCT) that is a non-invasive imaging modality generating micrometer resolution, two-dimensional (2-D) cross-sectional images and three-dimensional (3-D) volumetric data on the internal structure of optically scattering and reflective tissues [4, 5]. OCT is usually an **near-infrared interferometric technique**, in which depth information is revealed from the frequency analysis of the interferometric fringes (Fig. 1). The cross-sectional images, called B-scans, consist of a series of depth profiles (A-scans), that represent distribution of light scattering vs. depth. Combining multiple B-scans enables 3-D reconstruction of the structure of the imaged object. Although OCT is now a standard clinical imaging modality in ophthalmology for the detection and treatment monitoring of macular degeneration, retinopathy and glaucoma, scanning the anterior eye is still considered investigational.

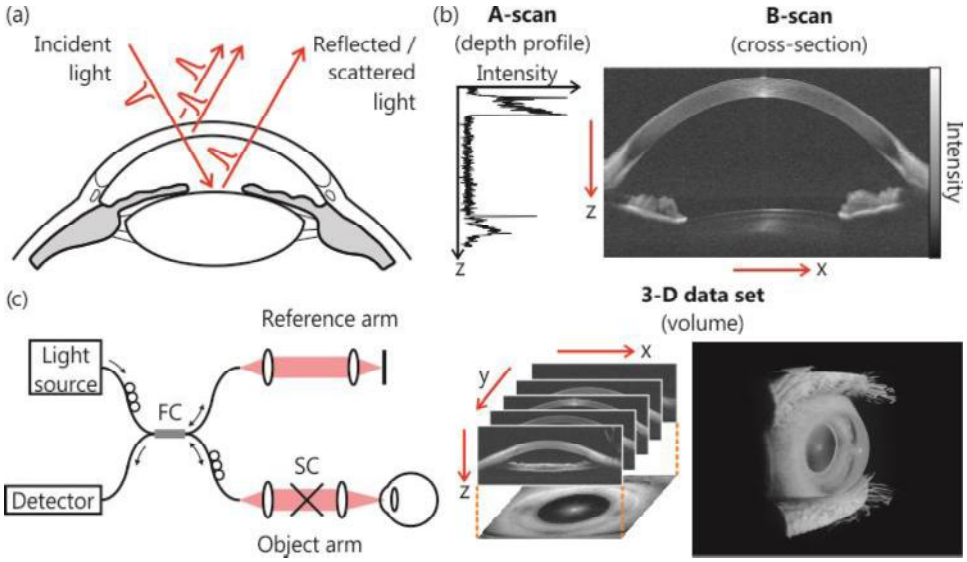

Figure 1. Optical coherence tomography. (a) Principle of OCT operation. (b) OCT image (B-scan) is composed of adjacent A-scans. Volumetric image enables 3-D reconstruction of the internal structure of the object. The nomenclature of the images is similar to that used in ultrasonography. (c) Scheme of simple OCT set-up (FC – fiber coupler, SC – scanners). Reproduced from [II.D.1].

V.2. Scientific challenges and scientific aims

The following **scientific hypothesis** was formulated for the proposed research: 2-D and 3-D infrared interferometric imaging enables precise measurements of the shape and distances in the eye as well as profilometry of the optical elements.

The objective of the studies that I performed was to develop the methodology enabling extraction of precise quantitative information on the geometrical features of complex optical systems based on near interferometric imaging data. This aim was accomplished on two tracks: (1) development of prototype laboratory set-ups and validation of their performance and (2) development

of software tools to extract morphometric quantitative information on the eye (OCT biometry) as well as on optical elements used for restoration of visual acuity (OCT microprofilometry).

The anterior segment of the eye has specific properties that make the OCT imaging challenging. Different aspects of OCT imaging, specific for *in vivo* visualization of the anterior segment of the eye, pose technical limitations and determine the development of laboratory and clinical anterior segment OCT systems [II.D.1].

Clinical applications can be enabled only for *in vivo* imaging that aims at **visualization of the eye in its natural state**. The movements of the eye facilitated by the extraocular muscles make the eyeball possible to be both shifted in all three directions and rotated. Additionally, some ocular structures like the crystalline lens change their positions and shapes during accommodation. Since the eye is in a constant motion, imaging of the ocular structures requires the acquisition time to be short enough to minimize the impact of ocular motility [6]. This can be realized by **high imaging speed** defined by high A-scan rate so that the data acquisition can be shortened. Consequently, the advances in imaging speed are critical for a precise and accurate extraction of quantitative parameters of the anterior segment of the eye. Clinical practice shows that the acquisition of OCT data should not exceed 2-3 seconds in order to assure both acceptable image quality and comfort of the patient during scanning.

Another important aspect of the imaging is associated with the anterior segment spatial dimensions that define the optically sampled volume for proper three-dimensional visualization. Anterior segment is **relatively large morphological structure** compared to the retina, especially in terms of axial direction. If we consider intraocular distances as well as the average refractive indices of human ocular media (cornea and aqueous), the **axial imaging range** of the OCT set-up should be at least 6 mm. What is more, average anterior chamber width of the eye determines transverse scan range to be at least 13 mm. The above-mentioned estimations indicate that scanning ca. ~13 mm × 13 mm × 6 mm volume is necessary to visualize the entire anterior chamber in all three dimensions spanning from the limbus to limbus and from the apex to at least the front of the crystalline lens. This in turn leads to **very large data sets** containing information on the anterior segment structures [7]. Keeping the transverse scanning density constant, imaging of the anterior segment of the eye with standard scan protocol means at least 4× larger scan area than in retinal imaging. It also indicates 4× bigger data set. This challenge can be partially solved by **development of specific scanning protocols** that account for the symmetry of the front part of the eye [8].

Optical imaging modalities require light to penetrate the tissue in order to generate the image. The anterior segment of the eye is composed of tissues that have different scattering properties, and

optimum light delivery to deeper layers depends on the wavelength of the light source. A proper design of the OCT system for anterior segment imaging should be equipped with the light source that provides **sufficient light penetration**. The choice of operating wavelength is a primary importance if one wants to image through highly scattering tissues like sclera. Light scattering dominates in the near infrared spectral region, which limits penetration depth. Since light absorption and scattering of most tissue components decrease with the illumination wavelength, higher penetration depth can be achieved with light at 1310 nm compared with light at 840 nm. On the other hand, the absorption of the vitreous humor, mainly composed of water, increases very rapidly for near infrared light. Consequently, it does not allow light at longer wavelengths to reach the retina [9]. Although anterior segment imaging prefers wavelength region around 1310 nm, the challenge of light source choice comes from the fact that other factors coming from the specific applications of OCT imaging should be also taken into account (e.g. resolution).

Optical inhomogeneity of the anterior segment components causes the OCT images to be distorted. Those **distortions** come from the fact that OCT measures optical rather than geometric distances. Moreover, light refraction occurs due to different values of the refraction indices of the cornea, the aqueous, and crystalline lens. Therefore, physical properties of the eye imply that the OCT images do not reveal the anterior chamber morphology correctly. The true morphology of the eye can be obtained from the OCT data when **additional complex image post-processing steps** are applied. Biometric information on the corneal topography requires **light refraction correction of the OCT data** [10].

To conclude, the AS-OCT instrument should feature the following parameters: high acquisition speed, sufficient penetration depth, relatively long imaging depth range, homogenous resolution (beam spot size) over the entire sampled volume and ability to generate the maps of internal surfaces of ocular structures (quantitative 3-D imaging). Imaging the anterior segment of the eye requires a combination of those capabilities to obtain clinically useful information. It is also worth to note that similar challenges appear when one wants to image non-biological objects, especially those which cause light refraction during light penetration.

However, the development of novel instrumentation cannot be achieved without gaining the knowledge about the fundamental limitations regarding the methodology. Therefore, I tried to address the above-mentioned aspects of the OCT imaging in a series of publications to develop optimized scanning instrument as well as to obtain precise and accurate quantitative data. My publications were written as the response to the considerable interest in the implementation of new technologies in

Fourier-domain OCT imaging. **Consequently, the specific aims of the studies included answers to the following questions:**

- How to design the optimized OCT instrument for anterior segment imaging? How different OCT technologies impact image quality and performance of anterior segment imaging?
- How the wavelength of the instrument affects image quality?
- How can we extend imaging depth range in OCT? Is it possible to image through the entire eye length?
- How to extract quantitative information on the structure of the eye from OCT?
- What are the limitations of precision and accuracy of biometric measurements using OCT data?
- Is it possible to apply the developed algorithms in other fields of science and technology?

V.3. Results

The development of Fourier-domain detection enabled a breakthrough in OCT imaging sensitivity and speed. Fourier-domain detection is based on capturing the spectral interference fringes in wavelength (wavenumber) domain by acquisition of multiple (usually of the order of thousands) spectral channels with no need for scanning the reference mirror. The information on the depth positions of particular reflection / scattering events (echo time delays) is coded in the oscillation frequencies of the obtained interference spectrum. The echo magnitude and time delay can be extracted from the received interferometric signal by its Fourier transformation [11]. The highest frequency that can be measured by the detection system defines the imaging depth range of OCT. The performance advantages of Fourier-domain OCT were recognized independently by several research groups in 2003 [12-14]. In general, Fourier-domain OCT achieves ~20 dB higher sensitivity than previous generation OCT systems with time domain detection enabling ~50 to 100 times faster imaging [15]. This feature makes OCT more feasible in clinical applications, and allows for significant development of the OCT technique.

- ***Anterior segment imaging with SD-OCT and CMOS line-scan camera technology***

The first implementation of Fourier-domain detection is based on a spectrometer with line-scan detector. In this approach, called Spectral / Fourier-domain OCT (SD-OCT), one-dimensional array detector enables simultaneous (parallel in time) measurement of all spectral components. The spectrometer design is responsible for the performance of this second generation of OCT technology. The imaging depth range in SD-OCT depends on the spectral resolution of the spectrometer (defined by a spectral range of a single spectral component), and the acquisition speed is determined by the repetition rate of the line-scan camera (i.e. reciprocal of a single camera exposition time). Nowadays, most current ophthalmic OCT instruments utilize SD-OCT technology.

In most cases the OCT instruments utilized CCD (Charge Coupled Device) technology [16]. However, in a paper [I.B.1], I implemented CMOS (Complementary Metal Oxide Silicon) technology and explored its usefulness in OCT imaging of the anterior segment of the eye. The aim of the study was to assess if CMOS detectors can be feasible for anterior segment OCT imaging. CMOS and CCD technologies differ in the way that signals are converted from signal (accumulated) charge to an analog signal and finally to a digital signal. In CCDs, the charge is transported through the chip, and sent out to the A/D converter that is placed outside the sensor. In contrast, in CMOS cameras, the front end of this data path is massively parallel since each pixel has a dedicated conversion electronics. CCD cameras designed specifically for near-infrared light are usually more sensitive than CMOS imagers.

I performed the comparative study which showed that whereas CMOS and CCD achieve the same level of shot noise limited sensitivity, the CMOS detector saturates for lower values of reference arm reflectivity than CCD. Such a noise characteristics of the detector indicates that lower levels of light power enable achieving shot-noise limited operation of the CMOS detector. The properties of CMOS cameras make them also well suited as the detectors in anterior chamber imaging because CMOS line-scan camera enables flexible choice of active pixels influencing both examination time and number of voxels, which is not possible in SD-OCT systems based on CCD cameras. In [I.B.1], I have demonstrated that such a flexibility in acquisition speed can be achieved by selecting lower number of pixels being read-out, which enhances the spectrum of imaging modes from high-resolution, high-definition cross-sectional imaging to high-speed (up to 135 kA-scans/s) volumetric imaging in time (so called 4-D imaging = 3-D + time) of eye dynamics. It has to be pointed out that it was an important step in technology development since higher speed enables *in vivo* imaging as well as reduction of artifacts due to the eye motions during scanning.

The system utilized light generated by a superluminescent diode in the range around 840 nm. The choice of the light source provided high axial resolution. However, higher scattering at 840 nm compared with light at 1 μm or 1.3 μm made the penetration of light into tissue shallower, which could be noticed especially when anterior chamber angle was imaged.

One of the limitations of SD-OCT is significant signal drop with depth, which is caused by the finite spectral resolution of the detection unit (finite size of the camera pixels). This roll-off can be partially reduced by a proper positioning of the object vs. focal plane of the interface and the zero delay plane of the interferometer. I demonstrated that positioning of the eye vs. focal plane and zero delay line has significant impact on image quality. Moreover, our studies showed the sensitivity limits to

visualize anterior segment structures (such as anterior chamber, crystalline lens, and anterior chamber angle with ciliary body), as illustrated in Fig. 2.

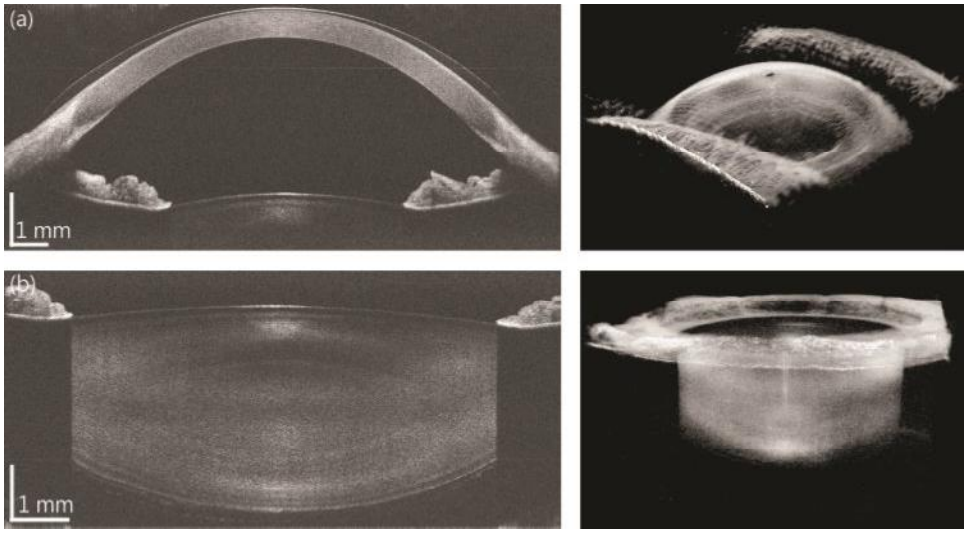

Figure 2. SD-OCT imaging of the anterior chamber of the eye with a prototype SD-OCT system at 840 nm. (a) High-definition cross-sectional image of the anterior chamber of the myopic eye with a contact lens. 3-D rendering of volumetric data set. (b) Cross-sectional image of the crystalline lens. 3-D rendering of volumetric data set. Reproduced from [I.B.1].

In fact, the paper [I.B.1] was the first demonstration of flexible line-scan CMOS detector in anterior segment OCT. The system has been deployed to the Instituto de Óptica "Daza de Valdés" at Consejo Superior de Investigaciones Científicas (CSIC) in Madrid and serves as an imaging tool till now. The results utilizing the system were published in few publications, and were subject to numerous presentations at the conferences [10, 17-20]. Moreover, the proposed design is often considered as a reference for other research groups [21-23].

- ***Smart velocity ranging in OCT by dedicated scanning protocols***

Assessing ocular blood flow *in vivo* is an important research area because many ocular diseases, such as diabetic retinopathy, glaucoma and age-related macular degeneration, are associated with alterations in retinal blood flow. Doppler OCT methods as interferometric modalities enable direct access to phase and can measure the speed of moving scatterers, such as red blood cells [24]. Physiologically, the blood flow values can differ significantly if one considers different vessels of either retinal or choroidal vascular networks. If one takes into account the fact that the angle of the vessels has significant impact on observed axial velocity component, the latter ranges from a fraction to several tens of millimeters per second. However, in a standard procedure the maximum axial velocity is determined by the A-scan rate (inversely proportional to the exposure time of the detector in SD-OCT), and its minimum limit can be estimated by phase noise assessment [25]. Therefore, it is desirable to develop

approaches that would be able to detect both slow and fast flows in the biological object. The challenge that I address is to achieve a flexible and wide velocity bandwidth in Doppler optical coherence tomography without lengthening acquisition speed and sacrificing image quality.

In a paper [I.B.2], I developed and demonstrated a method of visualization of flows with high dynamic range with high-speed OCT imaging by means of application of specific scanning protocols during acquisition. The approach can be called **velocity ranging** since it enables extraction fast and slow flows from a single SD-OCT data set. Depending on data processing approach, it is possible to enhance sensitivity of velocity detection to the particular velocity range. The scanning is performed in a way that the transverse range is divided into short B-scans (segments) in various configurations. I applied precise and accurate flow phantom with a glass capillary and a solution of scattering medium (Intralipid) to evaluate the feasibility of the idea (Fig. 3). I also demonstrated cross-sectional and volumetric imaging of the retinal vascular system using developed velocity ranging technique.

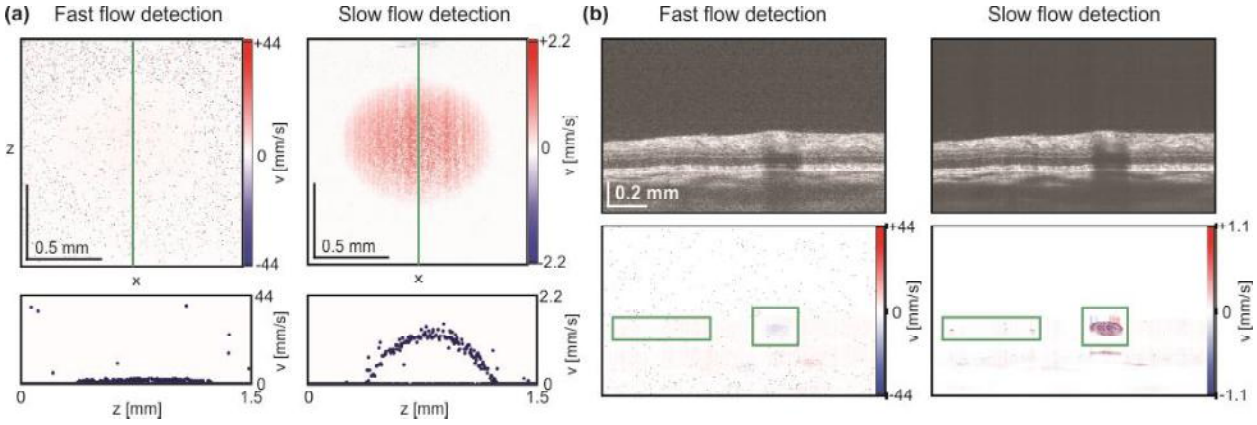

Figure 3. Velocity ranging in OCT. (a) Cross-sectional imaging of the glass capillary with flowing scatterers. The flow was set to axial velocity of 1.4 mm/s. The data set was processed to obtain sensitivity to fast flow (velocity range v_{max} = ±44.0 mm/s), and to slow flow (velocity range v_{max} = ±2.2 mm/s). (b) Cross-sectional imaging of the human retina. The data set was processed to obtain sensitivity to fast flow (velocity range v_{max} = ±44.0 mm/s), and to slow flow (velocity range v_{max} = ±1.1 mm/s). Small retinal vessels can be visualized in slow flow detection mode. Reproduced from [I.B.2].

The approach presented in [I.B.2] was the first demonstration of slow flow measurements in the human retina. It also stimulated research on retinal capillary network imaging, and has been widely used by many groups with further hardware improvements [26-28]. Similar approach can be used to reduce speckle noise in OCT images [29].

- ***Comprehensive eye characterization using ultrahigh speed swept source OCT with vertical-cavity surface emitting lasers. Full eye imaging as a new imaging mode***

The newest (third) generation of Fourier-domain OCT instruments is based on wavelength swept light sources (Swept source / Fourier-domain OCT; SS-OCT, known also as optical frequency domain imaging). The swept laser is a form of tunable light source, in which periodic tuning of spectrally narrow wavelength is provided. In SS-OCT, the interferometric signal (fringe) is acquired in time when the laser is sweeping the wavelength. The light is detected by a high-speed point photodetector and digitized by a data acquisition board (analog-to-digital card), which reconstruct the spectral fringes acquired over one frequency sweep of the light source. In other words, consecutive (serial in time) measurement of spectral channels is performed. Similar to SD-OCT, the echo delays or axial scans can be generated by Fourier transforming the detector signal [6].

Swept light source generates instantaneous temporally coherent electromagnetic radiation. However, the emitted light is temporally incoherent when the entire sweep is considered, as demanded by OCT. Wavelength-swept lasers utilize different tuning mechanisms and are considered to be a key technology for SS-OCT. The tuning technologies include: scanning mirror with grating, dispersion prism, rotating polygon, electro-optic deflector, Fabry-Perot filter (optionally with MEMS), distributed Bragg reflector etc. [30-32]. Recent advances include miniaturization of laser cavity, which improves both the tuning speed and coherence properties [33-37]. The important light source parameters for SS-OCT include: rapid sweep repetition rates over a wide frequency/wavelength range, single longitudinal mode operation (narrow instantaneous linewidth) for long coherence length, low excess noise and adjustable laser operation parameters.

Working at M.I.T. I applied a new swept source technology based on MEMS-tunable vertical cavity surface-emitting laser (VCSEL) operating at 1060 nm in SS-OCT. Unlike conventional edge-emitting laser diodes, VCSEL emits light perpendicular to the active region. The VCSEL consists of a multi-quantum well active layer between two highly reflective mirrors. The bottom mirror is an oxidized multi-quantum well distributed Bragg reflector (DBR). Together with a dielectric top mirror suspended on an electrostatic MEMS actuator, this forms a microcavity. Active region of the VCSEL is optically pumped, and wavelength tuning is performed by electrostatic deflection of the MEMS-tunable mirror [38].

I explored the following features of the first MEMS-tunable VCSEL operating at central wavelength of 1050 nm for ophthalmic imaging:

- Long coherence length

VCSEL operates with a single longitudinal mode instead of multiple modes (no mode hopping) and therefore has an extremely narrow instantaneous linewidth, which results in long instantaneous coherence length. Within available resources, we estimated that the coherence length is not shorter than 200 mm. I also compared the instantaneous coherence length of VCSEL with other swept lasers available on the market. The measurements shown in [I.B.3] show that VCSEL's coherence length is at least ~10x longer than that of competing swept source laser technology (Fig. 4a).

- High sweep rate

  MEMS mirror can be deflected by applying the voltage signal. The small size and high mechanical resonance frequency of the MEMS structure enable high sweep speeds and sweep repetition rates, which directly translates into high imaging speeds of SS-OCT. As an example, I demonstrated the retinal imaging with different acquisition speeds up to 580 kA-scans/s that enabled obtaining motion-free volumetric data sets of human retina *in vivo*.

- Adjustability of both the sweep rate and wavelength sweep range

  The maximum depth range (i.e. maximum fringe frequency) available by the acquisition system depends on the tuning range, sweep rate and the bandwidth of the detection system. VCSEL can offer tunability of the sweep rate and the wavelength sweep range so that MEMS-tunable VCSELs can serve as platform for the exploration and demonstration of multiple applications (Fig. 4b). I showed that both VCSEL and SS-OCT technology can be successfully integrated in the all-in-one instrument for ophthalmic imaging. Operating modes included high-speed high resolution retinal imaging, high-speed anterior segment imaging and full eye length (long-range) imaging.

It is possible to include all imaging modes mentioned here due to the fact that light centerd at 1060 nm were used. The light in that spectral range penetrates the tissue better than light in 840 nm range. On the other hand, the light is not as strongly absorbed as light in the range around 1310 nm. Consequently, the imaging of both anterior and posterior segments of the eye at 1060 nm seems to be an optimum solution although axial resolution can be a little bit worse.

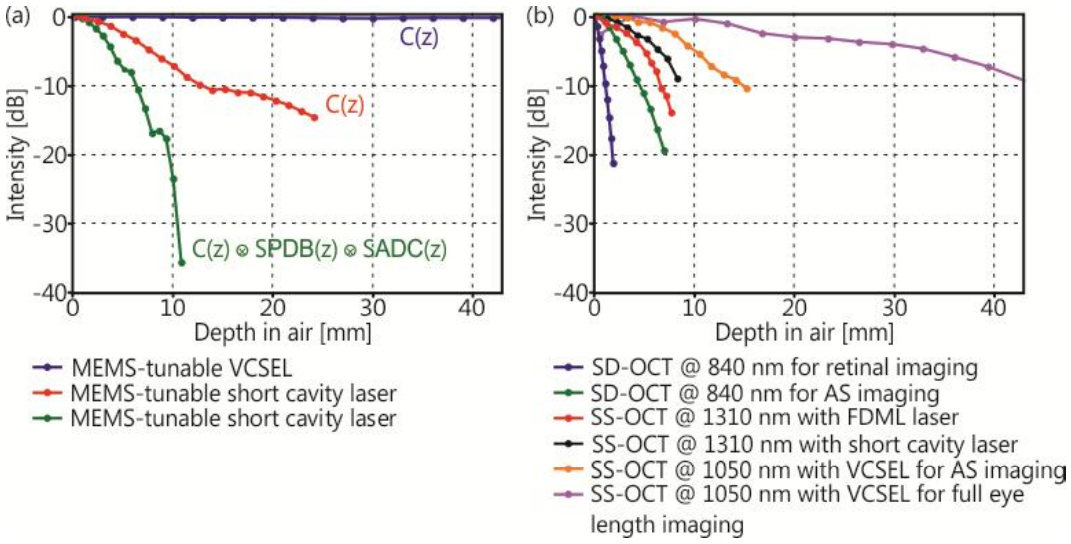

Figure 4. Coherence properties of swept light sources used in SS-OCT imaging. (a) Coherence functions for two light sources operating at central wavelength of 1050 nm. The impact of the frequency characteristics of both photodetector and acquisition card is provided. (b) Signal roll-off for laboratory OCT systems with Fourier-domain detection. Typical signal drop for retinal SD-OCT instrument is given for comparison. Reproduced from [I.B.1, I.B.3, I.B.4, I.B.5].

Full eye length imaging demonstrated for the first time in [I.B.3] is a form of long-range OCT imaging mode (Fig. 6a)**.** Due to the telecentric beam scanning, the eye optics enables visualization of anterior segment structures, whereas retinal signal from a single point (if no aberrations are present) can be observed.

- ***Reproducibility of a Long-Range Swept-Source Optical Coherence Tomography Ocular Biometry System and Comparison with Clinical Biometers***

OCT images do not represent geometrical structures, thus it is not possible to **directly** obtain any quantitative information on the morphological details of the object. In order to perform reliable OCT-based biometry, the distortion in OCT images must be corrected to obtain anatomically correct structural images. Generally, optical distortions can be classified in two groups:

a) system-specific distortions

System-specific distortions stem from non-ideality of optical components due to design and technical limitations. Distortions inherent to the system can occur during lateral beam scanning and corrections should be applied prior to biometric measurements. This issue has been well-addressed in previous references [10].

b) object-specific distortions

Image distortions can also be related to the optical inhomogeneity of the object imaged, which influences light propagation in the object. In the case of the eye, light refraction determines the

direction of beam propagation and therefore affects the intraocular distances measured from OCT images which display "optical paths". Therefore, the correct physical shape of anterior segment morphology can only be obtained after using refraction correction algorithms. I developed simple 2-D and advanced 3-D refraction correction algorithms for OCT data based on ray-tracing methods as well as algorithm to extract clinically useful parameters. Representative results of algorithm performance is shown in Fig. 5. The refraction correction algorithm assumes specific refractive indexes of the media between refracting surfaces. It is necessary to find the incidence angle for each refracting layer, which enables determination of refraction angle based on Snell's law.

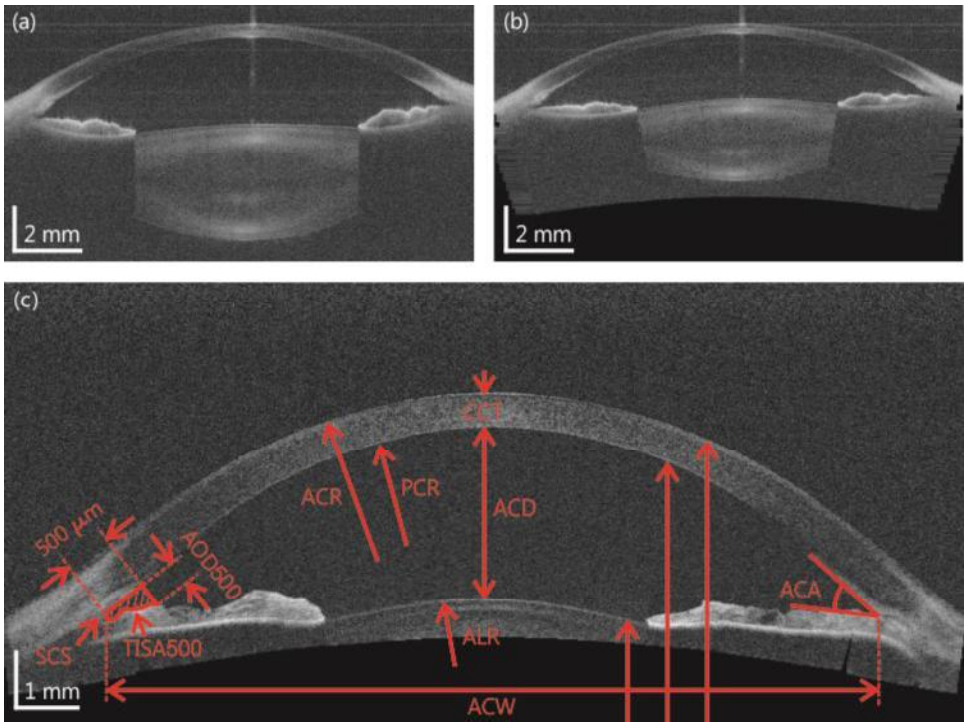

Figure 5. Cross-sectional image before (a) and after (b) refraction correction. (c) Quantitative analysis of the shape and dimensions of the anterior chamber of the eye. CCT – central corneal thickness, ACD – anterior chamber depth, ACR – anterior corneal radius of curvature, PCR – posterior corneal radius of curvature, ALR – anterior lens radius of curvature, ACW – anterior chamber width, ACA – anterior chamber angle, AOD500, TISA500 – other parameters describing the angle. Partially reproduced from [I.B.3].

The natural next step in development of presented full-eye-length SS-OCT imaging was the demonstration of possibility to extract quantitative information from OCT data sets in that imaging mode. In particular, the operational mode of long-range imaging can be very useful in ophthalmology to determine intraocular distances. The measurement of intraocular distances of the eye, known as **ocular biometry**, is essential for accurate outcomes in cataract and keratorefractive surgeries. Precisely measured axial intraocular distances are important for proper intraocular lens (IOL) power calculation.

Currently, ocular biometry with ultrasound is a gold standard in ophthalmology, especially when the eye with opacifications needs to be checked. Ultrasound devices can perform axial length measurements with a resolution of ~100 µm. However, ultrasound techniques require contact of the eye by a transducer or with the acoustic medium in order to measure axial distance. The optical biometric methods based on partial coherence interferometry were also demonstrated, and commercial optical devices such IOL Master (Zeiss) and LensStar (Haag-Streit) were developed. The advantage of optical biometry is that it is noncontact and provides higher resolution (10-20 µm) than its ultrasound counterpart.

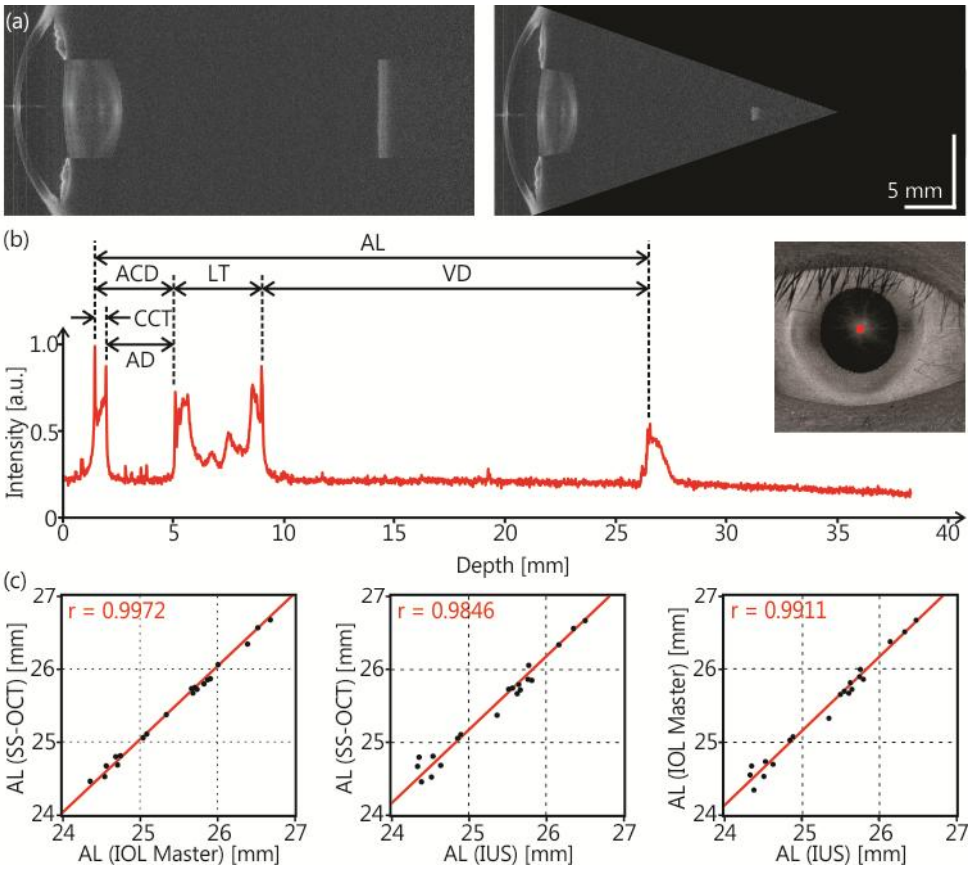

Figure 6. OCT ocular biometry. (a) Full-eye-length imaging (before and after refraction correction). (b) Extraction of intraocular distances from averaged central A-scan. (b) Comparison of SS-OCT ocular biometry with clinical biometric devices: IOL Master and immersion A-scan ultrasound biometer (IUS). Correlation coefficients are given as a measure of comparison. Reproduced from [I.B.4].

After demonstration of initial potential of the full-eye-length imaging mode to visualize the eye structures, translation of the method from laboratory to the clinic required additional experiments. Hence, I decided to design clinical study to demonstrate the feasibility of the proposed OCT-based ocular biometer. Accordingly, the aim of the study in paper [I.B.4] was to show reproducibility and

repeatability of the measurement of all intraocular distances from OCT data. To show the equivalence of the novel approach, comparison with clinical standards had to be performed. Therefore, SS-OCT ocular biometry was compared with two clinical biometers: immersion A-scan ultrasound biometer (Axis II PR, Quantel Medical Inc.) and gold standard optical biometer – IOLMaster (Carl Zeiss Meditec Inc.).

The precision and accuracy in axial eye length measurement are extremely important since that parameter is an important factor influencing IOL power estimation in all generations of IOL power calculation formulas. The error of 0.1 mm in axial length is equivalent to ~0.27 D error in the spectacle plane, when standard eye dimensions are assumed.

SS-OCT-based biometry performed in [I.B.4] demonstrates excellent reproducibility and repeatability with the axial length measurement precision not higher than 16 µm. This indicates that ocular biometry with the SS-OCT system showed precision comparable to the current gold standard clinical systems. In paper [I.B.4], I observed also a very good correlation of axial eye length measurements between SS-OCT, the IOL Master and immersion ultrasound, as given by statistical data analysis (ANOVA analysis) and Bland-Altmann method (Fig. 6). Additionally, the proposed technique is non-contact and it is well tolerated by the subjects in clinical setting. The longer wavelength (1.05 µm) used in the instrument may also enhance its performance in the cases of cataract patients, whose opacified lens usually prevents light to reach the retina. The studies in paper [I.B.4] formed a base for further development of the newest generation of optical biometers that use SS-OCT technology and possess additional imaging features with better light penetration for improved imaging capabilities in the cases of advanced cataracts. This research direction can be already observed in the literature [39, 40]. More information on applications of the proposed SS-OCT based optical biometry was given in Section V.4.

- ***High precision, high accuracy ultralong-range swept source OCT using VCSEL light source***

My previous papers [I.B.3-I.B.4] have shown that MEMS-VCSELs can be recognized as a versatile technology for many applications. Although I explored first applications of VCSEL technology in ophthalmic OCT imaging, the advantages of using tunable light sources with extended instantaneous coherence length can be also utilized in the applications other than biomedical. There are several industrial scenarios where 3-D long depth range imaging can serve as a tool for quality control of manufacturing processes.

In a paper [I.B.5], I illustrated several examples of long-range imaging that may be useful in non-biomedical applications. I demonstrated the longest ever imaging of 6-inch tall optomechanical component (post holder) (Fig. 7a)as well as imaging of the filament wire inside white (scattering) bulb or

a thick lens. I was also able to obtain ultralong depth ranges of the order of 1 m and to perform optical fiber length measurements using optical frequency-domain reflectometry (OFDR).

Profilometric characterization of surface topography with long-range OCT requires very accurate calibration of the system. Even small deviation of calibration from real values results in a large error at longer depths. Consequently, it is necessary to apply additional steps to obtain precise quantitative structural parameters. The application of laboratory (prototype) swept lasers may result in variations of tuning parameters between sweeps at different time scales (up to slow drift of wavelength tuning range and / or the central wavelength). Hence, sweep-to-sweep variations may lead to corresponding drift of imaging parameters, especially the axial (depth) range. In other words, initial calibration of the set-up may be no longer valid when imaging is performed. To address this issues, I tested several correcting approaches including: using fiber Bragg gratings (notch filters), additional Mach-Zehnder interferometers, two-channel detection etc.

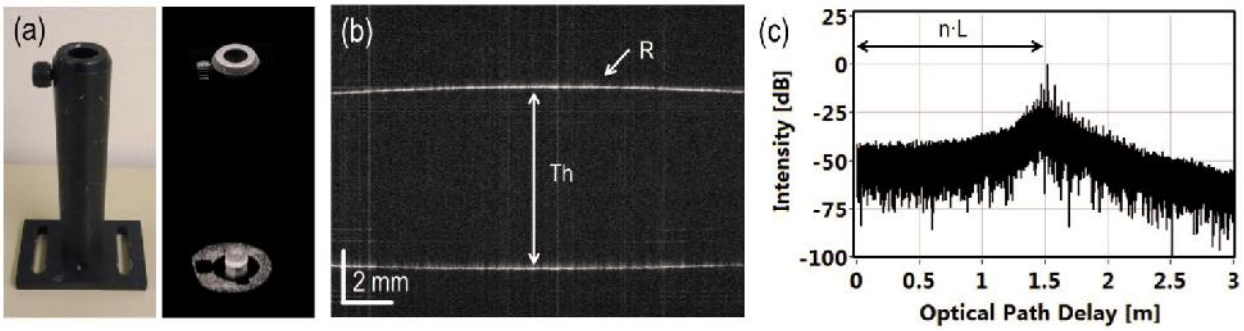

Figure 7. Long-range SS-OCT imaging and quantitative measurement. (a) Photograph (left) and 3-D reconstruction of volumetric OCT data set (right) of the optical post holder. (b) Cross-sectional image of a cylindrical lens enables measurement of central thickness *Th* and radius *R* of the surface curvature. (c) OFDR measurement of optical fiber length *L* (n = 1.4696). Reproduced from [I.B.5].

The application of light refraction correction algorithm allowed to extract information on the shape of the measured surfaces of the lens (Fig. 7b). The accuracy of the profilometric measurements was determined by comparing the mean measured value with a reference value, whereas the precision was evaluated using the standard deviation of the repeated measurements. Measurements of optical components show very good agreement between dimensions from OCT data and manufacturer specifications. Additionally, the fiber length was measured using OFDR method with the use of VCSEL light source (Fig. 7c).

The significance of the paper [I.B.5] comes from the fact that it is possible to obtain very precise shape and dimension measurements of the objects that are large or that are located at some long distance from the scanning unit.

- ***Quantitative optical inspection of contact lenses immersed in wet cell using swept source OCT***

The results obtained in the previous publication indicate that SS-OCT and algorithm for extraction of quantitative information from OCT data enable assessment of valuable properties of the objects such as contact lenses. The surface quality control of optical elements is especially important in determining the parameters of contact lenses. Measurements of soft contact lenses are difficult to be performed using standard methods. However, although OCT provides access to 3-D information with high resolution, it measures well scattering or reflecting surfaces. In most cases, the water content and material the contacts are made of do not allow for efficient measurement of both interfaces of the contact lenses. Therefore, Dr. Karnowski developed technique based on submerging in scattering medium, which allows obtaining images of high contrast. To extract precise information on topography of both surfaces of the lens, light refraction algorithm needs start with precise I applied the developed approach for light refraction correction to extract information on the shape of contact lenses. Since radial scan protocol was used during acquisition, a simplified version of light correction could be applied. In principle, if the beam scans through the apex of the lens, it is not necessary to consider out-of-plane light refraction. In other words, the phenomenon of light refraction during propagation through the object happens only in the plane of the obtained cross-section.

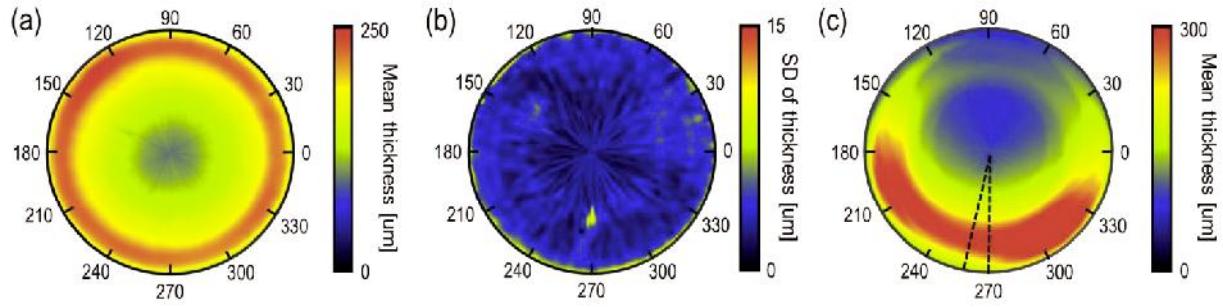

Figure 8. Quantitative contact lens evaluation. Averaged thickness map (a) and standard deviation map of the thickness (b) calculated from 10 measurements of the spherical soft contact lens. (c) Thickness map of the toric soft contact lens with clearly visible bottom weighting ballast. Circle of 9 mm diameter was chosen. Reproduced from [I.B.6].

In a paper [I.B.6], I combined the autopositioning method, the enhanced-contrast imaging, refraction correction to develop a new class of inspection instrument that allows for precise measurements of soft and hard contact lens metrology. The study showed that surface quality and the parameters of the soft contact lenses can be obtained with SS-OCT. The results can be regarded as an important step towards the development of methodology for optical inspection of transparent optical elements.

V.4. Possible applications

The results presented as the scientific achievement have in most cases direct applications in clinical practice as well in the industry. Firstly, four devices that I have developed operate in leading laboratories and ophthalmic clinics in Europe and the United States (Fig. 9):

a) Instituto de Óptica "Daza de Valdés" at Consejo Superior de Investigaciones Científicas (CSIC), Madrid, Spain (Fig. 9a);

b) University of Pittsburgh Medical Center, Pittsburgh, PA, USA (Fig. 9b);

c) New England Eye Center, Tufts University, Boston, MA, USA (Fig. 9c);

d) Laboratorio de Óptica, Universidad de Murcia, Murcia, Spain (Fig. 9e).

All prototypes serve as unique tools for validation of novel technologies in anterior segment or retinal OCT imaging or in OCT imaging of optical elements.

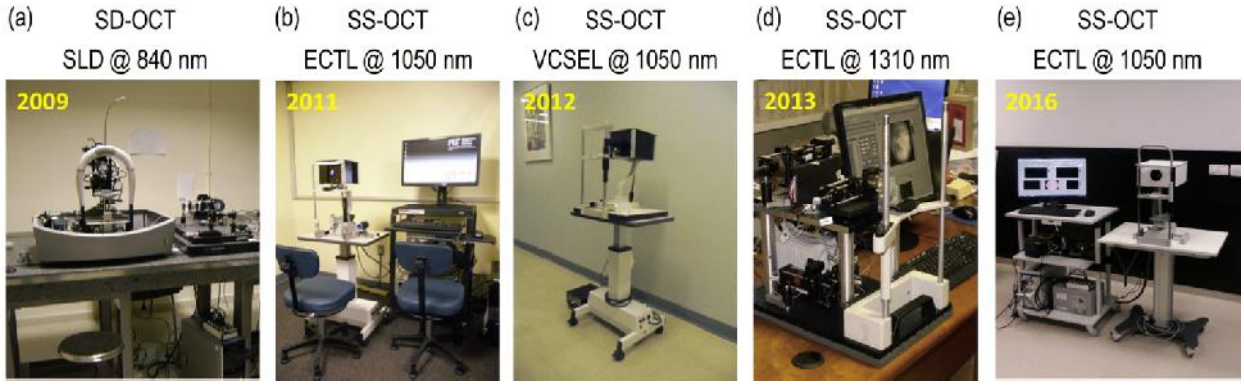

Figure 9. Prototype Fourier-domain OCT instruments developed by the author: (a) SD-OCT operating at 840 nm; (b) SS-OCT with short external cavity tunable laser (Axsun Technologies Inc.) operating at 1050 nm; (c) SS-OCT with prototype MEMS-tunable VCSEL (Praevium Inc. / Thorlabs Inc.) operating at 1050 nm; (d) SS-OCT with short external cavity tunable laser (Axsun Technologies Inc.) operating at 1310 nm; (e) long-range SS-OCT with customized short external cavity tunable laser (Axsun Technologies Inc.) operating at 1050 nm.

Future directions of technology development based on VCSEL-OCT will lead to a multi-purpose and highly functional instrument capable of eye imaging at previously unattainable speeds and imaging ranges. In particular, the long-range SS-OCT represents the next generation of ophthalmic OCT technology which offers superior performance compared with SD-OCT, the technology used in most standard clinical devices.

Secondly, the velocity ranging based segmented scan protocols have been later applied in many OCT angiographic techniques, that enabled visualization of fine vasculature in the retina. Although it is extremely hard to extract information on blood flow, first prototypes were already demonstrated to perform qualitative OCT angiography. It is currently a very promising field in ophthalmology.

Thirdly, quantitative data obtained from OCT-based biometry is of particular interest of clinicians. The algorithms of OCT image distortion correction and extraction of biometric parameters from OCT data can be used for future comparative studies with other well-established techniques. Ocular biometry based on SS-OCT has been already applied in commercial devices. Two of them – new version of IOL Master 700 and Argos – have been just approved by Food and Drug Administration (FDA) in the US (Fig. 10) and offer superior performance over existing biometers [39, 40]. They are based on similar approach, as presented by the author. Access to the volumetric structural data along with biometry will provide a platform for comprehensive high-resolution characterization of eye in different conditions.

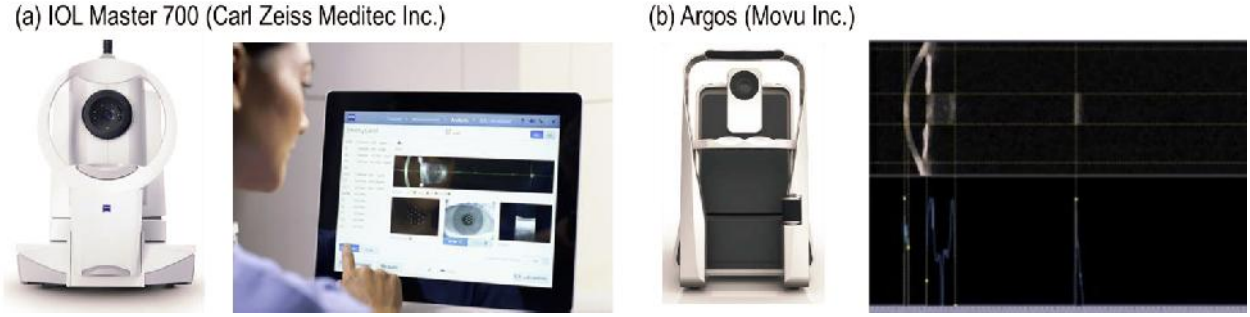

Figure 10. Commercial optical ocular biometers that have been FDA approved in 2015. Both IOLMaster 700 and Argos are based on similar principle as full-eye length SS-OCT and ocular biometry. Pictures taken from the web-sites of manufacturers.

Finally, precise and accurate measurements based on OCT can be used in industrial photonic applications like: fiber-optic testing, optical component characterization and profilometry. Optical 3-D non-contact profilometry has been widely used for 3-D sensing, mechanical engineering, machine vision and many other applications. Methods for accurate shape measurement are also important for product development and manufacturing quality control. The interferometry based on OCT principle is an ideal tool for remote sensing as well as for precise optical ranging. The characterization of contact lenses is an important step in quality control of manufacturing processes.

V.5. Summary and conclusions

To summarize, the scientific achievement demonstrated in the series of presented papers shows that:

- CMOS technology allows for higher flexibility in manipulation of imaging parameters in SD-OCT;
- new generation of tunable lasers makes it possible to adjust imaging parameters (e.g. imaging speed, resolution, depth range) to particular application;
- novel tunable light sources are characterized by long instantaneous coherence length and support achieving long imaging depth ranges that form a new class of medical and industrial applications;

- due to the properties of OCT technique it is necessary to include additional post-processing steps in order to extract quantitative information on the geometrical shape of the objects, i.e. light refraction correction;
- full eye length OCT imaging can be used to perform reproducible comprehensive ocular biometry, which correlates very well with established techniques;
- interferometric approached similar to SS-OCT enable precise determination of the shape (microprofilometry) of transparent optical elements used in the correction of vision defects.

VI. Description of other scientific achievements:

I was also involved in other projects that are partially related to the main topic of my scientific achievement. In this section, I will describe briefly some of other challenges I explored during my scientific career. Later on, I will demonstrate other activities as a researcher.

- ***Scleral and limbus imaging with SS-OCT***

As mentioned in Section V.3, OCT enables visualization flow of scattering particles (e.g. blood cells). Apart from the Doppler OCT methods that allow for calculations of velocity or flow in the vessels, there are also qualitative angiographic techniques, which display only the structure of vascular system. The latter methods are based on analysis the intensity fluctuations (speckle variations) due to the motion [41, 42]. Although it is generally believed that cornea is avascular, the peripheral anterior segment contains also vascular system in the conjunctiva and episclera. In a paper [II.C.1], I demonstrated application of high-speed swept source optical coherence tomography for vessel visualization in the limbus of the human eye. This region contains vessels that are associated with the circulatory system, lymphatic system and aqueous outflow system. I developed an intensity-based angiographic method that enhanced the differences in intensity images due to light attenuation in blood vessels.

- ***Quantitative assessment of oral mucosa and labial minor salivary glands in patients with Sjögren's syndrome and cystic fibrosis using swept source OCT***

Together with physicians from the Poznan University of Medical Sciences, I carried out a project regarding imaging of the mucosa of the lower lip and labial salivary glands in three cohorts: (1) patients with Sjögren's syndrome, (2) cystic fibrosis and (3) normal subjects (60 volunteers in total). The clinical hallmarks of both systemic diseases are associated with mucosal dysfunction and reduced or overly viscous secretions.

I developed a method called **OCT sialography** – an approach that enables optimal imaging of the labial salivary glands in conditions that the subjects consistently ranked as entirely comfortable. It is based on imaging through a sterile glass plate to enable proper exposition of the mucosa of the lower lip. The SS-OCT instrument operating at 1310 nm was developed, which assured good penetration of light into the tissue. The measurements were performed in the Department of Pediatric Gastroenterology and Metabolic Diseases in Poznań. In a paper [II.A.8], I demonstrated three-dimensional wide-field *in vivo* imaging of the mucosa of the lower lip and labial minor salivary glands in patients with Sjögren's syndrome and a control group. High quality volumetric images of the mucosa of the lower lip were clear until the depth of 800 µm, thus demonstrating comprehensive microarchitectural details. Moreover, access to 3-D data sets enabled quantitative description of the salivary glands: a set of morphometric parameters was therefore developed and applied. We observed larger volume of glandular tissue and its greater heterogeneity in patients with the most severe form of Sjögren's syndrome, which is suggestive of inflammation. Thus, the **OCT sialometry** (morphometry of the salivary glandular tissue) was demonstrated for the first time. Generally, the main advantage of the applied technique is its non-invasiveness that allows for 'optical biopsy'.

In the next article [II.A.2], we presented findings from an analogous investigation in cystic fibrosis patients and control subjects. The statistical analysis showed that surface density of the labial salivary glands was lower in patients than in age- and sex-matched healthy volunteers. The difference was large and described for the first time. Additional analyses of data from healthy volunteer groups of both studies revealed two confounding factors that should be controlled for in future clinical investigations employing OCT sialometry: age and body mass index [II.A.1].

- ***Ultrahigh-speed acousto-optic modulation for focus extension in optical coherence microscopy***

OCT enables depth-resolved imaging of the weakly scattering samples. Physical principle of OCT operation allows for decoupling of axial and transverse resolutions. The microscopic version of OCT, called optical coherence microscopy (OCM), utilizes tightly focused beam scanning the object. Therefore, depth-of-focus usually limits the axial imaging range in OCM, and it is difficult to image deeper structures with while maintaining high resolution. Accordingly, I addressed that issue by implementation of **dynamic focusing**. In paper [II.A.3], I developed tunable acousto-optic liquid lens (AOL) that enables ultra-fast dynamic focusing, and showed very good agreement between numerical simulations of the AOL performance and experimental results. I also proved that the degree of depth-of-focus extension depends linearly on the square of the focal length of the offset lens and on the amplitude of ultrasound. This is the feature enabling improvement of capabilities of imaging devices.

Since the device operates at the MHz frequency range, which is much higher than exposure rate of the camera in SD-OCT (acquisition speed), I proposed to use pulsed illumination synchronous with the frequency of ultrasound (stroboscopic illumination) to be able to perform time-resolved analysis of dynamic focusing on OCM image quality. The performance of the proposed approach was tested on reflecting and scattering phantoms as well as on the biological sample.

- ***Application of active optical elements for (quasi-)simultaneous imaging of the retina and the anterior segment of the eye***

The refractive property of the optical system of the eye prevents regular ophthalmic imaging devices to be able to image both anterior and posterior segment of the eye. This is due to the fact that either focused or collimated beam is projected on the cornea of the eye. I explore utilization of focus tuning elements (active optical elements) such as electro-optic tunable lenses to address this issue. Accordingly, I integrated the electro-optic tunable lens into the sample arm of the OCT instrumentation to test the performance of this approach. The studies showed that the proof-of-concept enables quasi-simultaneous visualization of anterior segment and the retina (data were already presented at 2016 Photonics West in San Francisco). After development of long-range OCT system that can image through the entire length of the eye, this is the next step that would lead to comprehensive imaging capability of OCT method.

- ***In vivo imaging cataract eyes and quantitative description of crystalline lenses with opacifications***

Cataract is nowadays one of the leading causes of blindness in human population and manifests in the opacification of the crystalline lens. The increase in light scatter in the lens reduces the image quality projected onto the retina, thus degrading vision. Surgical procedures aim at removal of opacified crystalline lens and implantation of the artificial intraocular lens. Important aspect of the whole procedure is to effectively visualize the opacifications in the crystalline lens in 3-D. OCT seems to be a good candidate since OCT maps light back-scattered from the internal structures, and therefore in cooperation with the Laboratorio de Óptica de la Universidad de Murcia (Prof. Pablo Artal) I developed the long-depth-range SS-OCT system operating at 1 μm that enables visualization of the entire anterior chamber. Comprehensive tests of different hardware solutions allowed for addressing the challenges such as: signal roll-off, homogenous illumination of the imaging volume, sensitivity etc. High sensitivity offered by SS-OCT enables imaging internal structure of the crystalline lens. During recent stay at Murcia I was able to image elderly people with no diagnosed cataract, and early signatures of the opacification in the lenses were found. Currently, I develop processing algorithm that will enhance contrast in

opacification cases and will enable cataract grading. The results will be presented at the ARVO Annual Meeting in Seattle (USA) this year.

- ***Other activities and achievements***

I have authored 31 peer-reviewed scientific papers in JRS list, 25 publications in journal not referenced in JRS or conference proceedings. My scientific record includes also 4 book chapters on OCT imaging of the anterior segment of the eye. My work has been cited in the scientific literature more than 600 times, giving the Hirsch factor of 12.

My scientific work is mainly focused on conducting research. Since 2006, I was involved in 14 projects, 5 of them as a Principal Investigator. Since 2008, when I joined the Medical Physics Group at the Institute of Physics, Nicolaus Copernicus University in Torun, my position is constantly covered by the external grants from Polish and American funding agencies. Therefore, my teaching responsibilities were considerably limited during that period. Although I had First Laboratory in Physics and exercises in Basics of Physics, when I was a PhD student at the Faculty of Mathematics, Physics and Informatics, University of Gdansk, However, after moving to Torun I was involved in teaching only occasionally (also for PhD students). Additionally, I mentored two undergraduate students and a student during his internship, and I reviewed couple of MSc / BSc theses. Currently, I am a mentor of two PhD students.

I actively participated in the conferences at both domestic and international level. I gave 38 talks and showed 4 posters at the conferences / congresses or during seminars in other scientific centers, and 13 of them were invited talks. When I include the presentations as an coauthor, the total number of presentations at the conferences increases to 88.

The results demonstrated here were obtained in two institutions: Institute of Physics of the Nicolaus Copernicus university in Toruń (Prof. Maciej Wojtkowski) and Massachusetts Institute of Technology (Prof. James G. Fujimoto). However, I have been collaborating also with other leading institutions on biomedical optics, ophthalmology and optometry, including: Collegium Medicum (Dr. hab. Barłomiej Kałuzny), Poznań University of Medical Sciences (Department of Pediatric Gastroenterology and Metabolic Diseases; Prof. Jarosław Walkowiak, Dr. Jan K. Nowak), Nencki Institute of Experimental Biology (Prof. Grzegorz Wilczyński), Oregon Health & Science University (Prof. David Huang), University of Pittsburgh Medical School (Prof. Joel S. Schumann, Dr. Gadi Wollstein, Dr. Larry Kagemann), New England Eye Center, Tufts University (Prof. Jay S. Duker), University of Murcia (Laboratorio de Óptica, Prof. Pablo Artal), Consejo Superior de Investigaciones Científicas (Instituto de Óptica, Visual Optics and Biophotonics lab, Prof. Susana Marcos).

During my scientific career, I pay special attention to serving the scientific society. Within this activity I reviewed ca. 100 manuscripts, serving for over 20 journals. In addition to that, I am an Associate Editor of *Open Physics* (De Gruyter Open), formerly *Central European Journal of Physics* (Versita & Springer). My tasks include promotional service for the papers published in *Open Physics* and occasionally management of submitted manuscripts. Moreover, I edited manuscripts in the *Journal of Ophthalmology* in 2015. Currently, I am also a member of Photonic Society of Poland, SPIE, Optical Society of America, The Association for Research in Vision and Ophthalmology, and the Club of the Foundation for Polish Science Scholars. As a PhD student, I represented PhD students in the Council of the Faculty of Mathematics, Physics and Computer Science of the University of Gdańsk (2005-2007). As a conference secretary, I was also involved in the organization of the 10th School on Acousto-Optics and Applications, that was held in Sopot in 2008.

I received numerous awards / scholarships for my work, including the Scholarship for Distinguished Young Scientists of the Polish Ministry of Science and Higher Education (2013); postdoc out-going Fellowship within the KOLUMB Programme of the Foundation for Polish Science (2010); Prof. M. Kwiek Award for Young Acousticians (2006) and several conference attendance grants that allowed me to participate in the international conferences (e.g. Foundation for Polish Science; Association for Research in Vision and Ophthalmology; International Commission for Acoustics / European Acoustics Association).

References

1. P. R. Griffiths and J. A. De Haseth, *Fourier transform infrared spectrometry* (John Wiley & Sons, 2007), Vol. 171.
2. J. D. Monnier, "Optical interferometry in astronomy," Rep. Prog. Phys. **66**, 789 (2003).
3. R. C. Youngquist, S. Carr, and D. E. N. Davies, "Optical coherence-domain reflectometry: a new optical evaluation technique," Opt. Lett. **12**, 158-160 (1987).
4. D. Huang, E. A. Swanson, C. P. Lin, J. S. Schuman, W. G. Stinson, W. Chang, M. R. Hee, T. Flotte, K. Gregory, C. A. Puliafito, and J. G. Fujimoto, "Optical Coherence Tomography," Science **254**, 1178-1181 (1991).
5. J. G. Fujimoto, "Optical coherence tomography for ultrahigh resolution in vivo imaging," Nat. Biotech. **21**, 1361-1367 (2003).
6. W. Drexler, M. Y. Liu, A. Kumar, T. Kamali, A. Unterhuber, and R. A. Leitgeb, "Optical coherence tomography today: speed, contrast, and multimodality," J. Biomed. Opt. **19**, 071412 (2014).
7. M. Gora, K. Karnowski, M. Szkulmowski, B. J. Kaluzny, R. Huber, A. Kowalczyk, and M. Wojtkowski, "Ultra high-speed swept source OCT imaging of the anterior segment of human eye at 200 kHz with adjustable imaging range," Opt. Express **17**, 14880-14894 (2009).
8. D. Huang, J. S. Duker, J. G. Fujimoto, B. Lumbroso, J. S. Schuman, and R. N. Weinreb, *Imaging the Eye from Front to Back with RTVue Fourier-Domain Optical Coherence Tomography* (Slack Inc., Thorofare, 2010), pp. 1-268.

9. S. L. Jacques, "Optical properties of biological tissues: a review," Phys. Med. Biol. **58**, R37-R61 (2013).
10. S. Ortiz, D. Siedlecki, I. Grulkowski, L. Remon, D. Pascual, M. Wojtkowski, and S. Marcos, "Optical distortion correction in Optical Coherence Tomography for quantitative ocular anterior segment by three-dimensional imaging," Opt. Express **18**, 2782-2796 (2010).
11. M. Wojtkowski, "High-speed optical coherence tomography: basics and applications," Appl. Opt. **49**, D30-D61 (2010).
12. R. Leitgeb, C. K. Hitzenberger, and A. F. Fercher, "Performance of fourier domain vs. time domain optical coherence tomography," Opt. Express **11**, 889-894 (2003).
13. M. A. Choma, M. V. Sarunic, C. H. Yang, and J. A. Izatt, "Sensitivity advantage of swept source and Fourier domain optical coherence tomography," Opt. Express **11**, 2183-2189 (2003).
14. J. F. de Boer, B. Cense, B. H. Park, M. C. Pierce, G. J. Tearney, and B. E. Bouma, "Improved signal-to-noise ratio in spectral-domain compared with time-domain optical coherence tomography," Opt. Lett. **28**, 2067-2069 (2003).
15. M. Wojtkowski, R. Leitgeb, A. Kowalczyk, A. F. Fercher, and T. Bajraszewski, "In vivo human retinal imaging by Fourier domain optical coherence tomography," J. Biomed. Opt. **7**, 457-463 (2002).
16. M. Wojtkowski, V. Srinivasan, T. Ko, J. Fujimoto, A. Kowalczyk, and J. Duker, "Ultrahigh-resolution, high-speed, Fourier domain optical coherence tomography and methods for dispersion compensation," Opt. Express **12**, 2404-2422 (2004).
17. A. de Castro, S. Ortiz, E. Gambra, D. Siedlecki, and S. Marcos, "Three-dimensional reconstruction of the crystalline lens gradient index distribution from OCT imaging," Opt. Express **18**, 21905-21917 (2010).
18. S. Ortiz, P. Perez-Merino, E. Gambra, A. de Castro, and S. Marcos, "In vivo human crystalline lens topography," Biomed. Opt. Express **3**, 2471-2488 (2012).
19. E. Gambra, S. Ortiz, P. Perez-Merino, M. Gora, M. Wojtkowski, and S. Marcos, "Static and dynamic crystalline lens accommodation evaluated using quantitative 3-D OCT," Biomed. Opt. Express **4**, 1595-1609 (2013).
20. P. Pérez-Merino, M. Velasco-Ocana, E. Martinez-Enriquez, and S. Marcos, "OCT-based crystalline lens topography in accommodating eyes," Biomed. Opt. Express **6**, 5039-5054 (2015).
21. M. X. Shen, L. L. Cui, M. Li, D. X. Zhu, M. R. Wang, and J. H. Wang, "Extended scan depth optical coherence tomography for evaluating ocular surface shape," J. Biomed. Opt. **16**, 056007 (2011).
22. M. Ruggeri, S. R. Uhlhorn, C. De Freitas, A. Ho, F. Manns, and J. M. Parel, "Imaging and full-length biometry of the eye during accommodation using spectral domain OCT with an optical switch," Biomed. Opt. Express **3**, 1506-1520 (2012).
23. C. Q. Zhou, J. H. Wang, and S. L. Jiao, "Dual channel dual focus optical coherence tomography for imaging accommodation of the eye," Opt. Express **17**, 8947-8955 (2009).
24. M. S. Mahmud, D. W. Cadotte, B. Vuong, C. Sun, T. W. H. Luk, A. Mariampillai, and V. X. D. Yang, "Review of speckle and phase variance optical coherence tomography to visualize microvascular networks," BIOMEDO **18**, 050901 (2013).
25. M. Szkulmowski, A. Szkulmowska, T. Bajraszewski, A. Kowalczyk, and M. Wojtkowski, "Flow velocity estimation using joint Spectral and Time domain Optical Coherence Tomography," Opt. Express **16**, 6008-6025 (2008).
26. S. Zotter, M. Pircher, T. Torzicky, M. Bonesi, E. Götzinger, R. A. Leitgeb, and C. K. Hitzenberger, "Visualization of microvasculature by dual-beam phase-resolved Doppler optical coherence tomography," Opt. Express **19**, 1217-1227 (2011).

27. Y. Jia, O. Tan, J. Tokayer, B. Potsaid, Y. Wang, J. J. Liu, M. F. Kraus, H. Subhash, J. G. Fujimoto, and J. Hornegger, "Split-spectrum amplitude-decorrelation angiography with optical coherence tomography," Opt. Express **20**, 4710-4725 (2012).
28. D. M. Schwartz, J. Fingler, D. Y. Kim, R. J. Zawadzki, L. S. Morse, S. S. Park, S. E. Fraser, and J. S. Werner, "Phase-variance optical coherence tomography: a technique for noninvasive angiography," Ophthalmology **121**, 180-187 (2014).
29. M. Szkulmowski, I. Gorczynska, D. Szlag, M. Sylwestrzak, A. Kowalczyk, and M. Wojtkowski, "Efficient reduction of speckle noise in Optical Coherence Tomography," Opt. Express **20**, 1337-1359 (2012).
30. S. R. Chinn, E. A. Swanson, and J. G. Fujimoto, "Optical coherence tomography using a frequency-tunable optical source," Opt. Letters **22**, 340-342 (1997).
31. S. H. Yun, G. J. Tearney, J. F. de Boer, N. Iftimia, and B. E. Bouma, "High-speed optical frequency-domain imaging," Opt. Express **11**, 2953-2963 (2003).
32. Y. Yasuno, V. D. Madjarova, S. Makita, M. Akiba, A. Morosawa, C. Chong, T. Sakai, K. P. Chan, M. Itoh, and T. Yatagai, "Three-dimensional and high-speed swept-source optical coherence tomography for in vivo investigation of human anterior eye segments," Opt. Express **13**, 10652-10664 (2005).
33. N. Fujiwara, R. Yoshimura, K. Kato, H. Ishii, F. Kano, Y. Kawaguchi, Y. Kondo, K. Ohbayashi, and H. Oohashi, "140-nm quasi-continuous fast sweep using SSG-DBR lasers," IEEE Photonics Technology Letters **20**, 1015-1017 (2008).
34. B. Potsaid, B. Baumann, D. Huang, S. Barry, A. E. Cable, J. S. Schuman, J. S. Duker, and J. G. Fujimoto, "Ultrahigh speed 1050nm swept source / Fourier domain OCT retinal and anterior segment imaging at 100,000 to 400,000 axial scans per second," Opt. Express **18**, 20029-20048 (2010).
35. K. Totsuka, K. Isamoto, T. Sakai, A. Morosawa, and C. H. Chong, "MEMS scanner based swept source laser for optical coherence tomography," Proceedings SPIE **7554**, 75542Q (2010).
36. M. P. Minneman, J. Ensher, M. Crawford, and D. Derickson, "All-Semiconductor High-Speed Akinetic Swept-Source for OCT," Proceedings SPIE **8311**, 831116 (2011).
37. V. Jayaraman, J. Jiang, H. Li, P. J. S. Heim, G. D. Cole, B. Potsaid, J. G. Fujimoto, and A. Cable, "OCT Imaging up to 760 kHz Axial Scan Rate Using Single-Mode 1310nm MEMS-Tunable VCSELs with > 100nm Tuning Range," in *2011 Conference on Lasers and Electro-Optics* (IEEE, 2011), 1-2.
38. V. Jayaraman, G. D. Cole, M. Robertson, C. Burgner, D. John, A. Uddin, and A. Cable, "Rapidly swept, ultra-widely-tunable 1060 nm MEMS-VCSELs," Electron. Lett. **48**, 1331-1333 (2012).
39. K. S. Kunert, M. Peter, M. Blum, W. Haigis, W. Sekundo, J. Schütze, and T. Büehren, "Repeatability and agreement in optical biometry of a new swept-source optical coherence tomography–based biometer versus partial coherence interferometry and optical low-coherence reflectometry," J. Cataract Refract. Surg. **42**, 76-83 (2016).
40. H. J. Shammas, S. Ortiz, M. C. Shammas, S. H. Kim, and C. Chong, "Biometry measurements using a new large-coherence length swept-source optical coherence tomographer," J. Cataract Refract. Surg. **42**, 50-61 (2016).
41. J. Fingler, R. J. Zawadzki, J. S. Werner, D. Schwartz, and S. E. Fraser, "Volumetric microvascular imaging of human retina using optical coherence tomography with a novel motion contrast technique," Opt. Express **17**, 22190-22200 (2009).
42. J. Enfield, E. Jonathan, and M. Leahy, "In vivo imaging of the microcirculation of the volar forearm using correlation mapping optical coherence tomography (cmOCT)," Biomed. Opt. Express **2**, 1184-1193 (2011).

dr Ireneusz Grulkowski